- Technical Paper -

NUMERICAL SIMULATION OF ULTIMATE CAPACITY OF STEEL PILE ANCHORAGE IN CONCRETE-FILLED STEEL BOX CONNECTION

Muhammad Aun BASHIR[*1], Kota NAKAYAMA [*2], Hitoshi FURUUCHI [*3] and Tamon UEDA[*4]

ABSTRACT

This paper presents the comparison of experimental and numerical analysis to determine ultimate capacity of steel pile anchorage in concrete filled steel box connection. In order to simulate the post peak behavior of the connection, a new equation for fracture energy of confined concrete is presented. The fracture energy equation is verified with more simple concrete filled steel tube cases and then installed in the FEM program. Based on the experimental results conclusion can be drawn that the load-deflection curve obtained from the simulation show good correlation with the experimental data.

Keywords: ultimate capacity, steel pile anchorage, concrete filled steel box connection, numerical simulation

1. INTRODUCTION

Steel concrete sandwich structure is a relatively new form of structural system. This form of structure has the potential to fully utilize respective strength of both steel and concrete with help of composite action such as confinement. It allows the prefabrication of large section in a factory, and enables rapid installation into main structure, dramatically reducing the fabrication cost and construction time. Steel faces act as permanent formwork during the construction and provide impermeable skins for the structure upon completion. So after considering these points, we selected steel box filled with concrete for connection between two structural members such as beam and foundation pile in a bridge. It has advantage over steel structure because of cost factor and it is a better option as compared to reinforced concrete connection due to strength and construction time. The purpose of our study is to present the numerical simulation of the experiments with the help of 3D nonlinear finite element program CAMUI developed by the author's laboratory [1].

The research on connection between steel beam and foundation pile by using concrete filled steel box was started by Emoto et al [2] and continued by Bashir et al [3]. The concrete filled steel box is a type of sandwich structure; however its failure mechanism is quite different from ordinary sandwich members. The major finding through both experimental and 3D-FEM numerical study by Emoto, et al. [2] was that failure of this connection occurs, when compression softening of concrete is caused by bearing stress from the steel pile. And other findings on shear connector effects was that the shear connector along the inserted length of pile enhanced the load carrying capacity of connection but shear connectors attached on skin plate of steel box had almost negligible effect on the strength of connection. The studies by Emoto et al. [2] and Bashir et al [3] showed the reliability of the 3D-FEM analysis. However, its reliability of predicting the peak load and post-peak behavior of the connection was not shown due to the fact that there were no experimental results of peak load.

The objective of this paper is to show the reliability of the FEM program analysis, for peak load and post peak behavior of the connection. So this program can provide cost effective solution over experimental alternatives to develop the design method of this type of connection. In order to achieve the target, a new constitutive model for confined concrete with fracture energy as a parameter is presented by trial and error method.

2. TEST PROGRAMS

Test specimen is the connection of the hybrid rigid frame bridge (Fig. 1). This type of connection as shown in Fig. 2 has been proposed due to construction conditions imposed to the bridge such as limited space. The rigid frame structure makes height of the beam shorter, while the connection, which is the concrete filled steel box, makes the abutment size smaller. Six specimens were tested. The notations S1 to S6 will be used for the test specimens. The principal variables among the test specimens were pile diameter, insertion length and pile thickness. The detail of experimental specimens is given in Table1. The steel box and steel beam dimension are same for all specimens. Fig. 4 presents the dimensions of the tested specimens.

*1 Doctoral Student, Graduate School of Engineering, Hokkaido University.
*2 Master Student, Graduate School of Engineering, Hokkaido University.
*3 Assistant Professor, Graduate School of Engineering, Hokkaido University, JCI Member.
*4 Professor, Graduate School of Engineering, Hokkaido University, JCI Member.

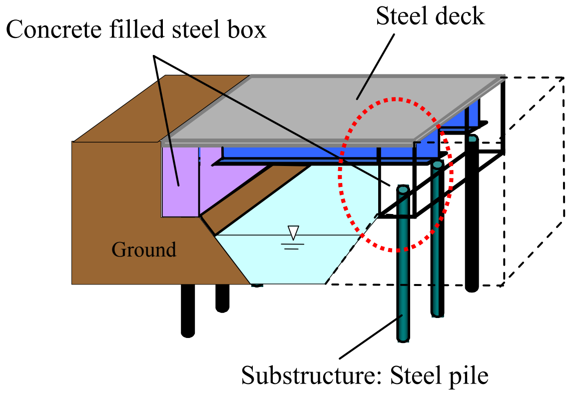

Fig 1. Hybrid rigid frame bridge

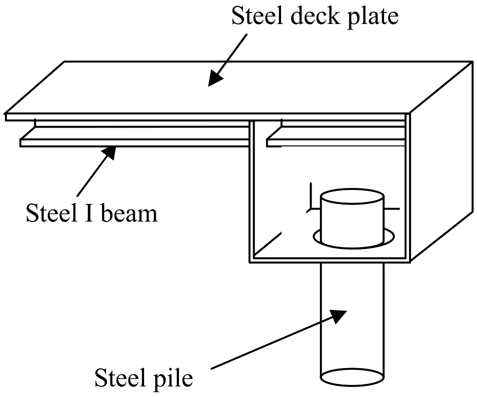

Fig 2. Connection of hybrid structure

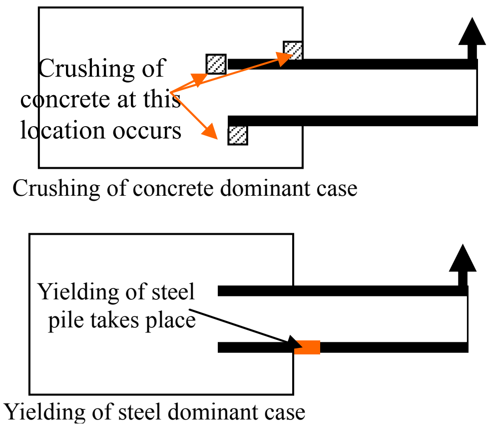

Fig 3. Failure mechanism

2.1 Test setup and instrumentation

The specimens were placed in such a position so that the pile was horizontal and steel beam was vertical. Monotonic downward vertical loading was applied to the pile at different pile length. Pile length is the length of pile outside the box up to the loading point. Steel beam was fixed at the bottom. Vertical displacement of pile and steel box was measured by using the displacement transducers. Strain gauges were attached to the pile inside the box and outside the box. Spacing between the strain gauges is 30 mm.

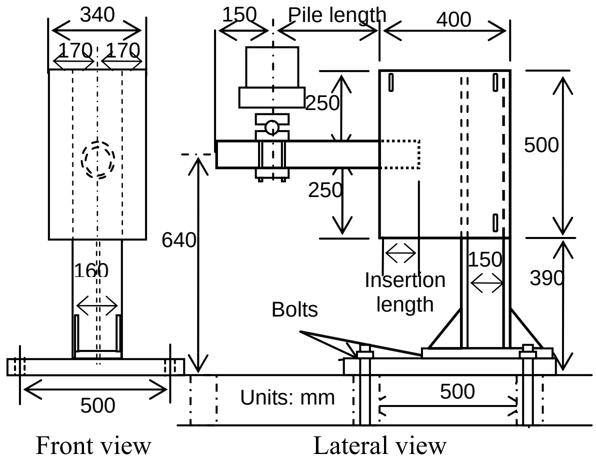

Fig.4 Specimen details

2.2 Test results

The experimental program included six specimens subjected to monotonic load perpendicular to the longitudinal axis of pile. The variable parameters are pile diameter, thickness, insertion length and pile length outside the steel box. Based on the experimental results two types of failure mechanisms were observed. Five specimens show that ultimate load capacity of the connection is controlled by yielding of pile steel. One specimen shows that crushing of concrete controls the failure of the connection. The specimen, failed by concrete crushing, shows ductile type of behavior after the peak load that is very strong feature of this type of connection. Failure mechanism cases are shown in Fig. 3.

3. FEM ANALYSIS

3.1 Analytical specimens

Same numbers of analytical specimens are prepared by using the commercially available software. The connection was symmetric along the longitudinal axis of pile. So in order to reduce the calculation time, half of the connection is modeled. 3D nonlinear finite element program CAMUI, developed by author's laboratory, was used to analyze the specimen. In order to simulate the ductile post peak behavior of the connection, a new equation for compressive fracture energy of confined concrete is presented by trial and error method. The fracture energy equation is verified with more simple concrete filled steel tube (CFT) cases and then installed in CAMUI.

Table 1 Specimen details

Specimen	Diameter (mm)	Insertion length (mm)	Pile length (mm)	Pile thickness (mm)	Steel box thickness (mm)	Concrete strength (MPa)	Steel box yield strength (MPa)	Steel pile yield strength (MPa)
S1	60.5	85	285	18	3	23.8	373	373
S2	60.5	103	256	4	3	23.8	373	373
S3	60.5	118	285	4	3	23.8	373	373
S4	60.5	130	285	18	3	23.8	373	294
S5	89.1	137	290	4.2	3	23.8	373	324
S6	34	140	285	4	3	23.8	373	327

3.2 Constitutive Model of Materials

(1) Constitutive law of concrete without crack

For un-cracked concrete and steel, elasto-plastic fracture model [4] is used. The elasto-plastic fracture model divides concrete nonlinearity into continuum damage and plasticity, and this model is also very suitable for steel. The adopted failure criteria that acted in agreement with Niwa's model [1] in tension-compression zone and Aoyagi and Yamada's model [1] in tension-tension region were extended to three-dimensional criteria by satisfying boundary conditions [4]. For cracked concrete until peak, Vecchio and Collins model [5] is used but for post peak, fracture energy concept was used [6]. Fracture energy concept will be modified to predict the post peak behavior of the confined concrete with steel. When crack occurs, a local coordinate system based on each crack plane is defined**.** In the case of 2 cracks occurring, two local coordinate systems arranged to share a parallel axis at the intersection line between the two crack planes. Constitutive models are applied in the direction parallel as well as normal to the crack and to shear slip along the crack planes. Global stresses are calculated by superposing the stress calculated in each local coordinate.

(2) Constitutive law of concrete with crack

The model is expressed as following relationship between σ, the tensile stress carried by concrete and δ, the crack opening displacement.

$$\frac{\sigma}{f_t} = \left\{1 + \left(c_1 \frac{\delta}{\delta_0}\right)^3\right\} \exp\left(-c_2 \frac{\delta}{\delta_0}\right) - \frac{\delta}{\delta_0}\left(1 + c_1^3\right)\exp\left(-c_2\right) \qquad (1)$$

Where,

c_1 : Constant 3 .00 (in normal concrete)

c_2 : Constant 6.93 (in normal concrete)

δ_0 : Limit crack opening , 140 mm

f_t : Axial tensile strength of concrete

The Vecchio and Collins model was applied for two dimensional concrete model in a plane parallel to the crack. This model is expressed as the relation between principal stress and principal strain. Compressive strength is reduced according to magnitude of tensile strain in the direction parallel to crack.

$$\sigma = f_c'\left[2\left(\frac{\varepsilon}{\varepsilon_0}\right) - \beta\left(\frac{\varepsilon}{\varepsilon_0}\right)^2\right] \quad \text{for } \varepsilon \le \varepsilon_p \qquad (2)$$

Where,

$\varepsilon_p = \varepsilon_o / \beta$

$\beta = 0.85 + 0.27\varepsilon_t / \varepsilon$

ε_t : Tensile strain in orthogonal to crack

ε_0 : Strain at compressive strength($2f_c/E_c$)

The model in the shear direction was designed based on the average shear stress-strain model in cracked concrete. Shear transfer model proposed by Li and Maekawa [7] was applied for the calculation of shear stiffness along a crack.

3.3 Bond link elements

Friction between steel and concrete was expressed by the bond link element with 16 nodes and 4 gauss point. The thickness of the element is considered zero. The following relationship of shear stress-slip of the friction taken from the result of the punching shear test by Inomata et al [8] was used in the FEM analysis.

$$\tau_{\max} = 0.578 \times \sigma \qquad (3)$$

Where,

$\tau_{\max}$: Shear stress

σ : Normal compressive stress

3.4 Modification of compression softening model for cracked concrete

The numerical solution of the finite element method using the smeared crack model is generally affected by the element size when the strain softening material model is adopted. This poses a severe problem to solve the post peak behavior of concrete structures. One solution of the problem was suggested by Nakamura [9] is to adjust the stress strain relation according to the fracture energy balance in terms of element size. This is, the fracture energy is treated as a material property and is kept constant in localized element regardless of element size. As we also know that post peak behavior of confined concrete varies with level of confinement. So by keeping these points in mind the fracture energy equation is modified in such a way that it should be a function of lateral confining stress. After peak stress, the effect of crack on compression softening is considered by the linear descending line. Reduced compressive stress has a limit that is 10% of the confined compressive strength. The gradient of strain softening is defined by compressive fracture energy.

$$G_{fc} = 8.8 \times (f'_{cc})^{(a + bf_l / f_c')} \qquad (4)$$

Where,

f'_{cc} : Confined concrete stress determined by Richart et al [10]

f_l : Lateral confining stress (average of two lateral stresses from 3D analysis)

Eq. (4) is modified form of Nakamura's equation [9]. The modification is change of f_c' to f'_{cc} and "0.5" is changed to variable form i.e. *(a +b f_l/ f_c')*. These two terms are modified because of following reasons. Fracture energy increases with the increase of confinement. The equation should be valid for both confined and unconfined concrete e.g. for confined concrete, the second term *(b f_l/ f_c')* will be added to "*a*" (because "f_l" will be compressive and sign convention is positive for compression). But on the other hand, for unconfined concrete, the second term *(b f_l/ f_c')* will be subtracted from "*a*" (because "f_l" will be tensile and sign convention is negative for tension).

"*a*" and "*b*" are the parameters which are determined by trial and error technique. In order to find "*a*" and "*b*" rather simple cases of confined concrete cases are chosen. Concrete-filled steel tube (CFT) cases subjected to axial compression are an ideal case to see the applicability of the post peak behavior with confinement. The limit strain for compression is calculated from Nakamura et al [9].

Table 2 Geometry and material properties of concrete filled steel tube columns

Column	B (mm)	t (mm)	B / t	Length (mm)	Steel tube fy (MPa)	Concrete fc' (MPa)	Tested by
Su-17	127	7.47	17	609.6	347	23.80	Schneider [11]
Su-29	127	4.34	29	609.6	357	26	Schneider [11]
Su-40	200	5	40	840	265.8	27.15	Huang et al [12]
Su-70	280	4	70	840	272.6	31.15	Huang et al [12]
Su-150	300	2	150	840	341.7	27.27	Huang et al [12]

$$\varepsilon_u = \frac{2G_{fc}}{\sigma_{peak} \times l_{eq}} + \frac{\varepsilon_p}{2} \quad (5)$$

$$\sigma = \sigma_{peak}\left[\frac{\varepsilon - \varepsilon_u}{\varepsilon_u - \varepsilon_d}\right] \quad (6)$$

Where,

ε_p : Compressive strain at peak stress.

σ_{peak} = $f'cc / \beta$ (β was already explained in Eq. 2)

l_{eq} = equivalent length, 40 mm which is element size.

Due to symmetry, only one eighth of the CFT are column is analyzed. Symmetric boundary conditions enforced on the symmetric planes. The corners of CFT with square sections are assumed to be exact 90° and corner radii are not considered. The uniform compressive loading in the y direction is applied to the top surface of the column directly. In this section, the experimental data from Schneider [11] and Huang et al [12] are used to calibrate the proposed fracture energy equation for confined concrete. The geometric and material properties of CFT columns are shown in Table 2. Specimens, that show concrete crushing dominant failure, are analyzed by varying the parameters "*a*" and "*b*" in the proposed fracture energy equation. In order to find the value of parameters "*a*" and "*b*", first of all value of "*b*" is assumed and "*a*" is varied. So in order to make our equation suitable for both confined and unconfined concrete, the value of "*b*" was assumed in such a way that $(a + b\, f_l / f_c')$ should become close to "0.5" value for unconfined concrete (Nakamura[9]). Parameters that precisely simulate the post peak behavior of confined concrete are selected and then verified for other specimens. Furthermore, it can be observed from Fig. 5, Fig. 6 and Fig. 7 that with the increase of confinement, post peak part of the load strain curve becomes more ductile. So it means fracture energy increases with increase of confinement level. This was the basic reason of the modification of the fracture energy equation. After analysis it can be observed from Fig.5, Fig. 6 and Fig. 7 that for $a = 0.86$, best simulation for post peak behavior of CFT column is achieved. So after trial and error method value of "*a*" and "*b*" were decided that is 0.86 and 7 respectively. After finding correct parameters two more CFT specimens were compared with available test data and found good corresponding between analytical and experimental results. This can be observed from Fig. 8 and Fig. 9. After analysis, it was also observed that value of bf_l / f_c' for the Su-17 (maximum confinement level case) at ultimate deformation was larger than that of Su-150 (minimum confinement level case). The value of bf_l / f_c' for both cases was 0.3 (7x1.02/23.8) and 0.01 (7x0.039/27.27) respectively. This is why post peak behavior of Su-17 was more ductile. f_l is the average of two lateral stresses calculated in the FE analysis.

3.5 Simulation of un-cracked concrete column.

For un-cracked concrete Elasto-Plastic Fracture (EPF) model is used for the simulation of post peak part of the stress strain curve. In order to verify the EPF model one specimen from previous study, that is unconfined concrete cylinder with aspect ratio 2 by Ahmad et al [13], is selected for comparison. After the analysis, good corresponding between analytical and experimental results is observed. It can be observed from Fig. 10.

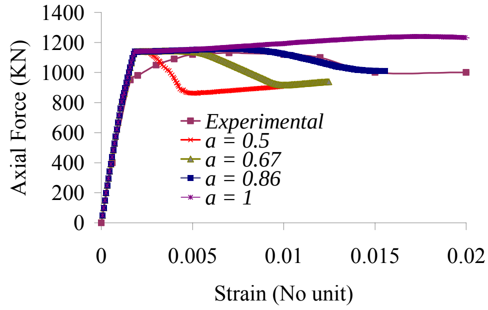

Fig.5 Axial force versus axial strain for Su-29

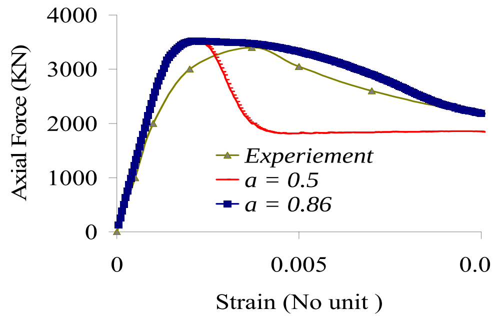

Fig.6 Axial force versus axial strain for Su-70

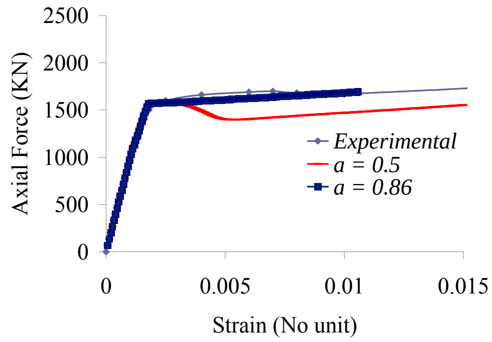

Fig.7 Axial force versus axial strain for Su-17

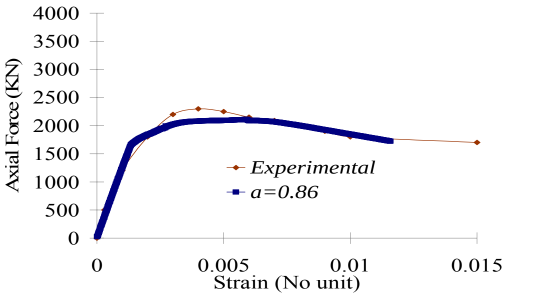

Fig.8 Axial force versus axial strain for Su-40

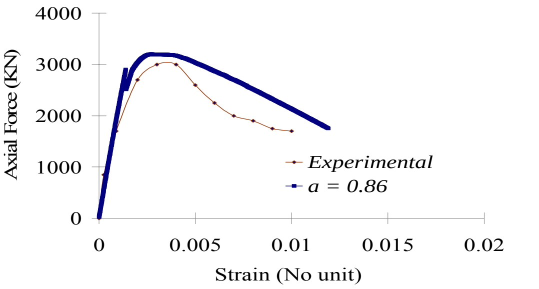

Fig.9 Axial force versus axial strain for Su-150

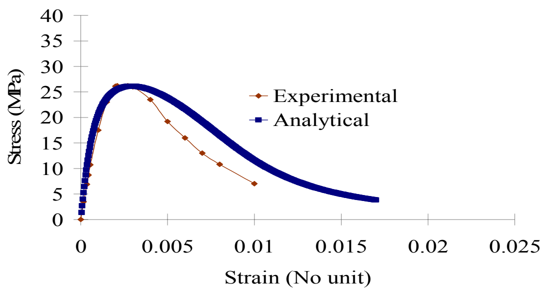

Fig.10 Stress versus strain for unconfined cylinder

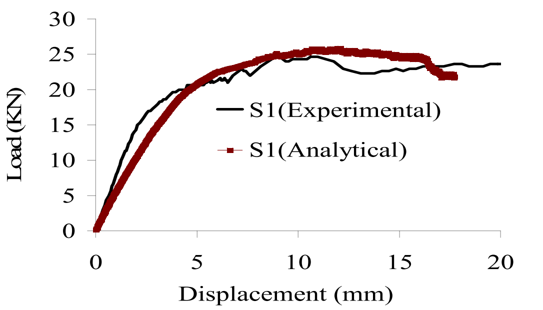

Fig. 11 Load displacement curve for concrete crushing case

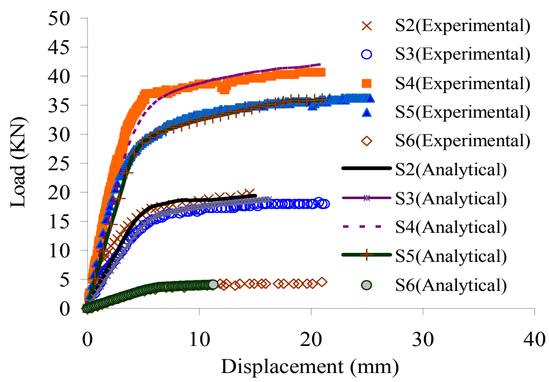

Fig. 12 Load displacement curve for steel pile yield case

4. Comparison of experimental and analytical results of pile anchorage of concrete filled steel box connection

After installing the modified fracture energy equation in CAMUI then we focused on numerical simulation of the experimental results of pile anchorage of concrete filled steel box connection. As the first step failure mechanisms of the connection were observed. Two types of failure mechanisms were observed. The first case is the crushing of concrete surrounding the pile and in the second type, yielding of steel pile controls the failure mode. Crushing of concrete is the dominant factor for the failure of the specimens S1 as shown in Fig. 11. From the figure it can be observed that experimental and analytical load displacement relationship shows good agreement. For specimens S2 to S6, the yielding of steel pile controls the failure mechanisms Fig. 12 shows that the experimental and analytical results are in good agreement in the load-displacement relationship.

5. Effect of confinement on pile anchorage strength of concrete filled steel box connection

In order to observe the effect of the confinement provided by the steel box on the load displacement curve of the connection, another specimen (S1_30) is analyzed. All dimensions of S1_30 are same as specimen S1 except the thickness of steel box. The thickness of steel box is changed from 3 mm to 30 mm in order to increase the confinement level of concrete surrounding the pile. In the analysis, it was observed that with the increase of thickness of steel box, load capacity of connection increases. This can be observed in Fig. 13. This increase of the load carrying capacity is because of the better confinement of the concrete surrounding the pile. Fig. 14 and Fig. 15 show the stress strain curve of different gauss point of same concrete element. The value of bf_l / f_c' at ultimate deformation, for gauss point in Fig. 15, for both cases was 0.29 and 0.12 respectively. It can be observed that peak stress, for larger box thickness, is higher than that of the case in which box thickness is small. That's why ultimate capacity of pile anchorage is increased.

6. CONCLUSIONS

(1) The modified fracture energy equation, for the simulation of post peak behavior of confined concrete, was presented. The modification was based on the concept that fracture energy of concrete in compression softening increases with the level of confinement. The modified equation is verified by the experimental data of concrete-filled steel tube.

(2) By using the concrete compression softening model with the modified fracture energy equation, the numerical simulation by 3D nonlinear finite element method (FEM) of experimental study to determine ultimate capacity of steel pile anchorage in concrete filled steel box connection was also

presented. Based on the experimental results conclusion can be drawn that the load- deflection characteristics obtained from the simulation show good correlation with the experimental data. Therefore this FEM program can be a cost effective tool to develop the design method of this type of connection.

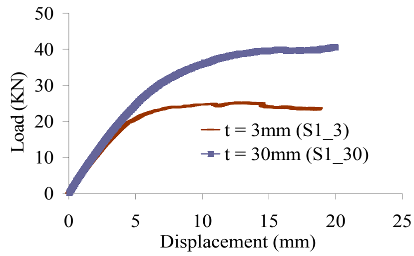

Fig. 13 Load deformation curve for different steel box thickness

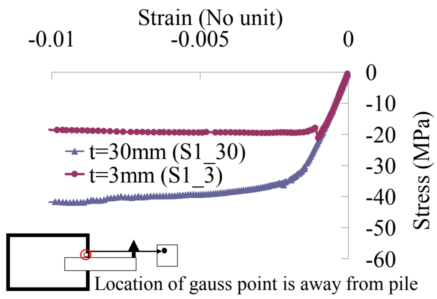

Fig. 14 Stress strain curve of gauss point of concrete for different steel box thickness

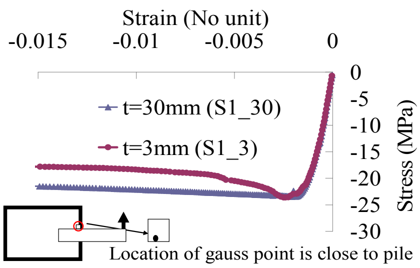

Fig. 15 Stress strain curve of gauss point of concrete for different steel box thickness

(3) Two types of failure mechanisms were observed i.e. crushing of the concrete surrounding pile and yielding of the steel pile. For concrete crushing dominant case, post peak behavior of the connection is very ductile that is the strong feature of this type of connection.
(4) The peak load of the connection increased with the increase of steel box thickness. This increase of peak load is because of the increase of confinement level of concrete surrounding the pile.

ACKNOWLEDGEMENT

The authors are very grateful to Japan Iron and Steel Federation (Education subsidy for steel structure research, 2005) for providing financial support to conduct our experimental work. The authors are grateful to Dr Yasuhiko Sato for his valuable advice towards this study and Mr. Tsutomu Kimura for his assistance in experimental work.

REFERENCES

[1] Takahashi, R., Sato, Y., Konno. K., and Ueda, T., “3D nonlinear punching shear simulation of steel concrete composite slab,” Journal of Advanced Concrete Technology, 3(2), 2005, pp.297-307
[2] Emoto, K., Furuuchi, H. and Ueda, T., “Analytical Study on Connection of Rigid-frame Bridge,” Proceedings of JCI, Vol.28, No.2, June 2006, pp.1339-1344
[3] Bashir, M. A., Furuuchi, H. and Ueda, T., “Parametric analysis of concrete filled steel box connection by using 3D finite element Analysis,” Journal of Structural Engineering, JSCE, Vol.54A, March, 2008, pp. 815-824
[4] Okamura, H. and Maekawa, K., “Nonlinear Analysis and Constitutive Models of Reinforced Concrete,” Gihodo Shuppan, 1991
[5] Takahashi, R. Sato, Y. and Ueda, T., “A Simulation of Shear Failure of Steel-Concrete Composite Slab by 3D Nonlinear FEM,” Journal of Structural Engineering,JSCE,Vol.48A,March, 2002, pp.1297 -1304
[6] Sato, Y., Tadokoro, T., and Ueda, T., “Diagonal tensile failure mechanism of reinforced concrete beams,” Journal of Advanced Concrete Technology, 2 (3), 2004, pp.327-341
[7] Li, B., Maekawa, K and Okamura, H., “Contact density model for stress transfer across crack in concrete,” Journal of Faculty of Engineering, University of Tokyo, Vol. 40(1),1998(B), pp.9-52
[8] Inomata, Y. et. al., “Static and Fatigue Bonding Behavior between Steel and Concrete Subjected to Bearing,” Proceedings of the 6th Symposium on Research and Application of Hybrid Structures (CD-ROM), JSCE, Nov., 2005, pp.(19-1)-(19-8), (In Japanese).
[9] Nakamura, H. and Higai, T., “Compressive fracture energy and fracture zone length of concrete,” Seminar on post peak behavior of RC structures subjected to seismic loads, JCI, Vol. 2, Oct., 1999, pp.259-272
[10] Richart, FE. Brandtzaeg, A., Brown, RL. “A study of the failure of concrete under combined compressive stresses,” University of Illinois Bulletin 185, 1928, p. 105
[11] Schneider, S. P., “Axially loaded concrete filled steel tubes,” J. Structural Eng., 124(10), 1998, pp.1125-1138
[12] Huang, C. S., et al., “Axial load behavior of stiffened concrete filled steel tubular columns,” J. Structural Eng., 128(9), 2002, pp.1222-1230
[13] Ahmad, S. H. Shah, S. P., “Stress strain curve of concrete confined by spiral reinforcement,” ACI Journal, Vol. 79,Nov.,1982, pp. 484-490